

UC San Diego

UC San Diego Previously Published Works

Title

MEAN-FIELD THEORY AND COMPUTATION OF ELECTROSTATICS WITH IONIC CONCENTRATION DEPENDENT DIELECTRICS.

Permalink

<https://escholarship.org/uc/item/3dz3x04h>

Journal

Communications in Mathematical Sciences, 14(1)

ISSN

1539-6746

Authors

Li, Bo
Wen, Jiayi
Zhou, Shenggao

Publication Date

2016

DOI

10.4310/cms.2016.v14.n1.a10

Peer reviewed



HHS Public Access

Author manuscript

Commun Math Sci. Author manuscript; available in PMC 2016 February 12.

Published in final edited form as:

Commun Math Sci. 2016 ; 14(1): 249–271. doi:10.4310/CMS.2016.v14.n1.a10.

MEAN-FIELD THEORY AND COMPUTATION OF ELECTROSTATICS WITH IONIC CONCENTRATION DEPENDENT DIELECTRICS *

BO LI[†], JIAYI WEN[‡], and SHENGGAO ZHOU[§]

[†] Department of Mathematics and Center for Theoretical Biological Physics, University of California, San Diego, 9500 Gilman Drive, Mail code: 0112, La Jolla, CA 92093-0112, USA. bli@math.ucsd.edu

[‡] Department of Mathematics and Center for Theoretical Biological Physics, University of California, San Diego, 9500 Gilman Drive, Mail code: 0112, La Jolla, CA 92093-0112, USA. j2wen@ucsd.edu

[§] Department of Mathematics and Center for Theoretical Biological Physics, University of California, San Diego, 9500 Gilman Drive, Mail code: 0112, La Jolla, CA 92093-0112, USA. s4zhou@math.ucsd.edu

Abstract

We construct a mean-field variational model to study how the dependence of dielectric coefficient (i.e., relative permittivity) on local ionic concentrations affects the electrostatic interaction in an ionic solution near a charged surface. The electrostatic free-energy functional of ionic concentrations, which is the key object in our model, consists mainly of the electrostatic potential energy and the ionic ideal-gas entropy. The electrostatic potential is determined by Poisson's equation in which the dielectric coefficient depends on the sum of concentrations of individual ionic species. This dependence is assumed to be qualitatively the same as that on the salt concentration for which experimental data are available and analytical forms can be obtained by the data fitting. We derive the first and second variations of the free-energy functional, obtain the generalized Boltzmann distributions, and show that the free-energy functional is in general nonconvex. To validate our mathematical analysis, we numerically minimize our electrostatic free-energy functional for a radially symmetric charged system. Our extensive computations reveal several features that are significantly different from a system modeled with a dielectric coefficient independent of ionic concentration. These include the non-monotonicity of ionic concentrations, the ionic depletion near a charged surface that has been previously predicted by a one-dimensional model, and the enhancement of such depletion due to the increase of surface charges or bulk ionic concentrations.

*This work was supported by the US National Science Foundation (NSF) through the grant DMS-131973, the NSF Center for Theoretical Biological Physics through the grant PHY-0822283, the US National Institutes of Health through the grant R01GM096188, and a UCSD Chancellor's Interdisciplinary Collaboratories grant.

Keywords

Electrostatic interactions; concentration-dependent dielectrics; mean-field models; Poisson–Boltzmann theory; generalized Boltzmann distributions; nonconvex free-energy functional; variational analysis; numerical computation

1. Introduction

Electrostatic interactions among charged solutes, mobile ions, and polarized solvent play an important role in the stability and dynamics of biological molecules in aqueous solution [4, 13, 16, 28, 29, 42–44, 53, 54]. Poisson’s equation and Poisson–Boltzmann (PB) equations are efficient mathematical descriptions of such interactions [3, 11, 13, 14, 19, 21, 24, 25, 36, 45, 53]. A basic hypothesis in such descriptions is that an underlying charged molecular system can be treated as a dielectric medium characterized by its dielectric coefficient that can vary spatially. Under normal conditions, the dielectric coefficient for water is close to 80, while that for proteins can be as low as 1–4 [26, 27]. Experiment and molecular dynamics (MD) simulations have indicated that the dielectric coefficient can depend on the local ionic concentrations [9, 10, 17, 26, 27, 31, 33, 40, 47, 50–52, 57, 58]. In this work, we use a mean-field variational approach to study how such dependence affects the equilibrium properties of electrostatic interactions in an ionic solution.

Consider an ionic solution near a charged surface. Assume there are M ionic species in the solution. (Typically $1 \leq M \leq 4$.) Denote by $c_i = c_i(x)$ the local ionic concentration of the i th species at a spatial point x . Our key modeling assumption is that the dielectric coefficient ε depends on the sum of local ionic concentrations of all individual ionic (either cationic or

anionic) species: $\varepsilon = \varepsilon(\bar{c}(x))$, where $\bar{c} = \sum_{i=1}^M c_i$. This dependence is qualitatively the same as that on the salt concentration. The latter can be constructed by fitting experimental or MD simulations data. Figure 1.1 shows the dependence of the dielectric coefficient on the concentration of NaCl [27, 40] and the fitted analytic form of such dependence. In general,

we assume that the function $\varepsilon = \varepsilon(\bar{c})$ is monotonically decreasing, convex, and is bounded below by a positive constant. Examples of such a function $\varepsilon = \varepsilon(\bar{c})$ are

$$\varepsilon\left(\frac{\bar{c}}{c}\right) = \frac{\alpha_0 - \alpha_1}{1 + \xi \frac{\bar{c}}{c}} + \alpha_1 \quad \text{and} \quad \varepsilon\left(\frac{\bar{c}}{c}\right) = (\alpha_0 - \alpha_1) e^{-\xi \frac{\bar{c}}{c}} + \alpha_1,$$

where all α_0 , α_1 , and ξ are constant parameters fitting experimental or MD simulations data with $\alpha_0 > \alpha_1 > 0$. Note that $\varepsilon(0) = \alpha_0$ and $\varepsilon(\infty) = \alpha_1$. We remark that the choice of \bar{c} instead of salt concentration reflects our attempt in understanding the contribution of each individual ionic species through its concentration to the dielectric environment, as biological properties are often ion specific (e.g., the ion selectivity in ion channels). Using $\bar{c} = \sum_{i=1}^M c_i$

allows us to input the concentration of each individual ionic species, and also to determine the variation of the free energy with respect to such individual ionic species.

The dielectric coefficient measures the polarizability of a material exposed to an external electric field. Due to their asymmetric structures, water molecules form permanent dipoles. They orient randomly in the bulk due to thermal fluctuations. Such orientational polarization makes the bulk water a strong dielectric medium. In the proximity of charged particles such as ions (cations or anions), however, water molecules are attracted by the charges, forming a hydration shell. These dipolar water molecules in the shell are aligned to the local electric field. Such saturation of local orientational polarizability leads to a weaker dielectric response of water near charges to the external electric field. Consequently, the dielectric coefficient in a region of high ionic concentrations is expected to be smaller than that in a region of lower ionic concentrations [7,15,22,27,57]. This dielectric decrement is one of the main properties of electrostatic interactions that we study here.

We now let the ionic solution occupy a bounded domain Ω in \mathbb{R}^3 with a smooth boundary Ω . We assume that the boundary Ω of Ω is divided into two nonempty, disjoint, and smooth parts Γ_D (D for Dirichlet) and Γ_N (N for Neumann); cf. Figure 1.2. (The case that $\Gamma_D = \emptyset$, i.e., $\Gamma = \Gamma_N$, can be treated similarly.) We also assume that we are given a fixed charged density $\rho_f : \Omega \rightarrow \mathbb{R}$, a surface charge density $\sigma : \Gamma_N \rightarrow \mathbb{R}$, and a boundary value of the electrostatic potential $\psi_\infty : \Gamma_D \rightarrow \mathbb{R}$. We consider minimizing the following mean-field electrostatic free-energy functional of the ionic concentrations $c = (c_1, \dots, c_M)$ [12, 20, 36, 48, 49]:

$$F [c] = \int_{\Omega} \frac{1}{2} \rho(c) \psi(c) dV + \int_{\Gamma_N} \frac{1}{2} \sigma \psi(c) dS + \beta^{-1} \sum_{i=1}^M \int_{\Omega} c_i \left[\log(\Lambda^3 c_i) - 1 \right] dV - \sum_{i=1}^M \mu_i \int_{\Omega} c_i dV. \quad (1.1)$$

Here, the first two terms together represent the electrostatic potential energy. In these terms, $\rho(c)$ is the total charge density, defined by

$$\rho(c) = \rho_f + \sum_{i=1}^M q_i c_i, \quad (1.2)$$

where $q_i = Z_i e$ with Z_i the valence of the i th ionic species and e the elementary charge, and $\psi = \psi(c)$ is the electrostatic potential determined as the solution to the boundary-value problem of Poisson’s equation [7, 30, 32]

$$\begin{cases} \nabla \cdot \varepsilon(\bar{c}) \varepsilon_0 \nabla \psi = -\rho(c) & \text{in } \Omega, \\ \varepsilon(\bar{c}) \varepsilon_0 \frac{\partial \psi}{\partial n} = \sigma & \text{on } \Gamma_N, \\ \psi = \psi_\infty & \text{on } \Gamma_D, \end{cases} \quad (1.3)$$

where ε_0 is the vacuum permittivity and ψ/n denotes the normal derivative at Γ with n the exterior unit normal. The third term in (1.1) represents the ionic ideal-gas entropy, where β^{-1}

$= k_B T$ with k_B the Boltzmann constant and T the absolute temperature, \log denotes the natural logarithm, and Λ is the thermal de Broglie wavelength. The last term in (1.1), in which μ_i is the chemical potential for the i th ionic species, represents the chemical potential of the system that results from the constraint of total number of ions in each species.

Our main contributions are as follows:

(1) We derive the first and second variations of the electrostatic free-energy functional (1.1). Setting the first variation to zero, we obtain the following generalized Boltzmann distributions that relate the equilibrium concentrations c_1, \dots, c_M to the corresponding electrostatic potential ψ :

$$c_i = c_i^\infty \exp \left\{ -\beta \left[q_i \psi + \frac{1}{2} \varepsilon' \left(\bar{c} \right) \varepsilon_0 |\nabla \psi|^2 \right] \right\}, \quad i=1, \dots, M, \quad (1.4)$$

where c_i^∞ is the bulk concentration of the i th ionic species that is determined by the parameters Λ and μ_i . Here we assume $\psi_\infty = 0$. A more general formula is given in Subsection 2.2. This formula was obtained in [7] for a one-dimensional system and a linear $\varepsilon = \varepsilon \left(\bar{c} \right)$. Note that if ε does not depend on the concentrations then $\varepsilon' \left(\bar{c} \right) = 0$, and we recover the classical Boltzmann distributions. If $\varepsilon = \varepsilon \left(\bar{c} \right)$ is linear in \bar{c} as assumed in [7, 27], then $\varepsilon' \left(\bar{c} \right)$ does not depend on \bar{c} and the equilibrium concentrations are uniquely determined by the potential ψ . In the general case, where $\varepsilon = \varepsilon \left(\bar{c} \right)$ is nonlinear in \bar{c} , the equilibrium concentrations are only defined implicitly by (1.4) through the potential ψ .

(2) We show by numerical calculations that there are possibly multiple values of concentrations $c = (c_1, \dots, c_M)$ that can depend on the same potential ψ through the generalized Boltzmann distributions. We also construct some examples to prove that the free-energy functional can be indeed nonconvex.

(3) We minimize numerically our electrostatic free-energy functional for a radially symmetric system of both counterions and coions. By our extensive numerical computations, we find several interesting properties of the electrostatic interactions attributed to the dependence of dielectric on ionic concentrations. These include the depletion of ions near a charged surface that has been previously described by a one-dimensional model with a linear $\varepsilon = \varepsilon \left(\bar{c} \right)$ [7], the non-monotonicity of ionic concentrations near such a surface, and the shift of peaks of the ionic concentration profiles due to the increase of surface charges or bulk concentrations.

Our free-energy functional (1.1) extends those in [12, 20, 36, 49], where the dielectric coefficient is independent of concentrations, and that in [7], where the dielectric coefficient depends linearly on the concentrations. A nonlinear dependence of dielectric coefficient on concentrations is significant, as it can lead to the existence of multiple equilibrium

concentrations. Our numerical results show interesting phenomena, extending those found in [5, 7, 22, 31, 34]. We notice that several authors have studied the dielectric decrement and related issues through the polarization of solvent molecules and ions [1, 5, 6, 22, 46].

We organize the rest of the paper as follows: In Section 2, we derive the first variations of the free-energy functional and the generalized Boltzmann distributions. In Section 3, we derive the second variations of the free-energy functional. In Section 4, we show by numerical calculations that the generalized Boltzmann distributions can lead to multiple values of concentrations. We also show by examples that the free-energy functional is in general nonconvex. In Section 5, we minimize numerically the mean-field electrostatic free-energy functional for a radially symmetric system. Finally, in Section 6, we draw our conclusions.

2. First Variations and Generalized Boltzmann Distributions

Unless otherwise stated, we assume the following throughout the rest of the paper:

(A1) The dielectric coefficient function $\varepsilon \in C^1([0, \infty))$. It decreases monotonically and is convex. Moreover, there are two positive numbers ε_{\min} and ε_{\max} such that

$$\varepsilon_{\min} \leq \varepsilon \left(\frac{\cdot}{\bar{c}} \right) \varepsilon_{\max} \quad \forall \bar{c} \geq 0; \quad (2.1)$$

(A2) The set $\Omega \subset \mathbb{R}^3$ is bounded, open, and connected with a smooth boundary $\Gamma = \partial\Omega$ (e.g., Γ is in the class C^2). The boundary $\partial\Omega$ is divided into two disjoint, nonempty, and smooth (e.g., in the class of C^2) parts Γ_D and Γ_N ;

(A3) The functions $\rho_f : \Omega \rightarrow \mathbb{R}$, $\sigma : \Gamma_N \rightarrow \mathbb{R}$, and $\psi_\infty : \Gamma_D \rightarrow \mathbb{R}$ are all given. Moreover, $\rho_f \in L^\infty(\Omega)$, σ is the restriction of a $W^{1,\infty}(\Omega)$ -function (also denoted by σ) on Γ_N , and ψ_∞ is the restriction of a $W^{1,\infty}(\Omega)$ -function (also denoted by ψ_∞) on Γ_D .

Note that we use standard notation for Sobolev spaces [2, 18, 23].

We denote

$$\begin{aligned} H_{D,0}^1(\Omega) &= \{ \phi \in H^1(\Omega) : \phi=0 \text{ on } \Gamma_D \}, \\ H_D^1(\Omega) &= \{ \phi \in H^1(\Omega) : \phi=\psi_\infty \text{ on } \Gamma_D \}. \end{aligned}$$

Let $u \in L^1(\Omega)$. Suppose

$$\|u\| := \sup_{0 \neq \phi \in L^\infty(\Omega) \cap H_{D,0}^1(\Omega)} \frac{1}{\|\phi\|_{H^1(\Omega)}} \int_\Omega u \phi dV < \infty.$$

Since $L^\infty(\Omega) \cap H_{D,0}^1(\Omega)$ is dense in $H_{D,0}^1(\Omega)$, we can identify u as an element in $H_{D,0}^{-1}(\Omega)$, the dual space of $H_{D,0}^1$, and write $u \in H_{D,0}^{-1}(\Omega)$. We denote

$$X = \left\{ c = (c_1, \dots, c_M) \in L^1(\Omega, \mathbb{R}^M) : c_i \geq 0 \text{ a. e. } \Omega, i=1, \dots, M; \sum_{i=1}^M q_i c_i \in H_{D,0}^{-1}(\Omega) \right\}.$$

Let $c \in X$. It follows from the Lax–Milgram Lemma and the Poincaré inequality for functions in $H_{D,0}^1(\Omega)$ [18, 23] that the boundary-value problem of Poisson’s equation (1.3) has a unique weak solution $\psi = \psi(c)$, defined by $\psi \in H_{D,0}^{-1}(\Omega)$ and

$$\int_{\Omega} \varepsilon(\bar{c}) \varepsilon_0 \nabla \psi \cdot \nabla \phi dV = \int_{\Omega} \rho(c) \phi dV + \int_{\Gamma_N} \sigma \phi dS \quad \forall \phi \in H_{D,0}^1(\Omega). \quad (2.2)$$

Similarly, we define $\psi_D = \psi_D(c) \in H_D^1(\Omega)$ to be the unique weak solution to

$$\begin{cases} \nabla \cdot \varepsilon(\bar{c}) \varepsilon_0 \nabla \psi_D = 0 & \text{in } \Omega, \\ \varepsilon(\bar{c}) \varepsilon_0 \frac{\partial \psi_D}{\partial n} = 0 & \text{on } \Gamma_N, \\ \psi_D = \psi_{\infty} & \text{on } \Gamma_D, \end{cases} \quad (2.3)$$

defined by $\psi \in H_{D,0}^{-1}(\Omega)$ and

$$\int_{\Omega} \varepsilon(\bar{c}) \varepsilon_0 \nabla \psi_D \cdot \nabla \phi dV = 0 \quad \forall \phi \in H_{D,0}^1(\Omega). \quad (2.4)$$

2.1. First variations

Let $c = (c_1, \dots, c_M) \in X$ and $d = (d_1, \dots, d_M) \in X$. We define

$$\delta F [c] [d] = \lim_{t \rightarrow 0} \frac{F [c+td] - F [c]}{t} \quad (2.5)$$

if $c + td \in X$ for $|t| \ll 1$ and the limit exists, and call it the first variation of $F [\cdot]$ at $c \in X$ in the direction d .

Theorem 2.1—Let $c = (c_1, \dots, c_M) \in X$. Assume there exist positive numbers δ_1 and δ_2 such that $\delta_1 < c_i(x) < \delta_2$ for a.e. $x \in \Omega$ and $i = 1, \dots, M$. Assume also that

$d = (d_1, \dots, d_M) \in L^{\infty}(\Omega, \mathbb{R}^M)$. Then

$$\delta F [c] [d] = \sum_{i=1}^M \int_{\Omega} d_i \delta_i F [c] dV,$$

where for each i ($1 \leq i \leq M$) the function $\delta_i F [c] : \Omega \rightarrow \mathbb{R}$ is given by

$$\delta_i F [c] = q_i \left[\psi (c) - \frac{1}{2} \psi_D (c) \right] - \frac{1}{2} \varepsilon' (\bar{c}) \varepsilon_0 \nabla \psi (c) \cdot \nabla [\psi (c) - \psi_D (c)] + \beta^{-1} \log (\Lambda^3 c_i) - \mu_i. \quad (2.6)$$

We shall identify $\delta_i F [c]$ defined in (2.6) as the the first variation of F at c in the i th coordinate direction. We note that our assumptions on $c_i(x)$ ($i = 1, \dots, M, x \in \Omega$) are expected to hold true for a local minimizer $c = (c_1, \dots, c_M)$. This can be argued using the same analysis in [35, 36], where perturbed, lower energy concentrations are constructed for the usual PB free-energy functional, based on the observation that the entropic change is larger than the potential change. To prove the theorem, we first prove the following:

Lemma 2.2—Under the assumption of Theorem 2.1, we have

$$\|\psi (c+td) - \psi (c)\|_{H^1(\Omega)} \rightarrow 0 \quad \text{and} \quad \|\psi_D (c+td) - \psi_D (c)\|_{H^1(\Omega)} \rightarrow 0 \quad \text{as } t \rightarrow 0.$$

Proof: Denote $\bar{d} = \sum_{i=1}^M d_i$. By the weak formulations for $\psi(c + td)$ and $\psi(c)$ (cf. (2.2)), and the definition of $\rho(c)$ (cf. (1.2)), we have for $\phi \in H_{D,0}^{-1}(\Omega)$ that

$$\begin{aligned} & \int_{\Omega} \left[\varepsilon (\bar{c} + t \bar{d}) - \varepsilon (\bar{c}) \right] \varepsilon_0 \nabla \psi (c+td) \cdot \nabla \phi dV + \int_{\Omega} \varepsilon (\bar{c}) \varepsilon_0 \nabla [\psi (c+td) - \psi (c)] \cdot \nabla \phi dV \\ &= \int_{\Omega} \left[\varepsilon (\bar{c} + t \bar{d}) \varepsilon_0 \nabla \psi (c+td) \cdot \nabla \phi dV - \int_{\Omega} \varepsilon (\bar{c}) \varepsilon_0 \nabla \psi (c) \cdot \nabla \phi dV \right. \\ &= \int_{\Omega} [\rho (c+td) - \rho (c)] \phi dV \\ &= t \sum_{i=1}^M \int_{\Omega} q_i d_i \phi dV. \end{aligned}$$

Setting $\phi = \phi_t := \psi (c+td) - \psi (c) \in H_{D,0}^1(\Omega)$, we then have by (2.1) that

$$\begin{aligned} & \varepsilon_{\min} \varepsilon_0 \int_{\Omega} |\nabla \phi_t|^2 dV \\ & \leq \int_{\Omega} \varepsilon (\bar{c}) \varepsilon_0 |\nabla \phi_t|^2 dV \\ & = t \sum_{i=1}^M \int_{\Omega} q_i d_i \phi_t dV - \int_{\Omega} \left[\varepsilon (\bar{c} + t \bar{d}) - \varepsilon (\bar{c}) \right] \varepsilon_0 \nabla \psi (c+td) \cdot \nabla \phi_t dV \\ & = t \sum_{i=1}^M \int_{\Omega} q_i d_i \phi_t dV - \int_{\Omega} \left[\varepsilon (\bar{c} + t \bar{d}) - \varepsilon (\bar{c}) \right] \varepsilon_0 |\nabla \phi_t|^2 dV \\ & \quad - \int_{\Omega} \left[\varepsilon (\bar{c} + t \bar{d}) - \varepsilon (\bar{c}) \right] \varepsilon_0 \nabla \psi (c) \cdot \nabla \phi_t dV \\ & \leq |t| \left(\sum_{i=1}^M |q_i| \|d_i\|_{L^2(\Omega)} \right) \|\phi_t\|_{L^2(\Omega)} + \varepsilon_0 \|\varepsilon (\bar{c} + t \bar{d}) - \varepsilon (\bar{c})\|_{L^\infty(\Omega)} \|\nabla \phi_t\|_{L^2(\Omega)}^2 \\ & \quad + \varepsilon_0 \|\varepsilon (\bar{c} + t \bar{d}) - \varepsilon (\bar{c})\|_{L^\infty(\Omega)} \|\nabla \psi (c)\|_{L^2(\Omega)} \|\nabla \phi_t\|_{L^2(\Omega)}. \end{aligned}$$

Since $\|\varepsilon \left(\bar{c} + t \bar{d} \right) - \varepsilon \left(\bar{c} \right)\|_{L^\infty(\Omega)} \rightarrow 0$ as $t \rightarrow 0$, we conclude by the Poincaré inequality applied to ϕ_t that there exists a constant $C > 0$ independent of t with $|t| \ll 1$ such that

$$\|\phi_t\|_{H^1(\Omega)} \leq C \left(|t| + \varepsilon_0 \|\varepsilon \left(\bar{c} + t \bar{d} \right) - \varepsilon \left(\bar{c} \right)\|_{L^\infty(\Omega)} \right) \rightarrow 0 \quad t \rightarrow 0.$$

This proves that $\|\psi(c+td) - \psi(c)\|_{H^1(\infty(\Omega))} \rightarrow 0$ as $t \rightarrow 0$. The proof of the convergence $\|\psi_D(c+td) - \psi_D(c)\|_{H^1(\Omega)} \rightarrow 0$ as $t \rightarrow 0$ is similar and simpler.

Proof: [Proof of Theorem 2.1] Let us write $F[c] = F_{\text{pot}}[c] + F_{\text{ent}}[c]$, where

$$F_{\text{pot}}[c] = \int_{\Omega} \frac{1}{2} \rho(c) \psi(c) dV + \int_{\Gamma_N} \frac{1}{2} \sigma \psi(c) dS, \quad (2.7)$$

$$F_{\text{ent}}[c] = \sum_{i=1}^M \int_{\Omega} \left\{ \beta^{-1} c_i \left[\log(\Lambda^3 c_i) - 1 \right] - \mu_i c_i \right\} dV. \quad (2.8)$$

By routine calculations (cf. [12, 35, 36]), we have

$$\delta F_{\text{ent}}[c][d] = \lim_{t \rightarrow 0} \frac{F_{\text{ent}}[c+td] - F_{\text{ent}}[c]}{t} = \sum_{i=1}^M \int_{\Omega} d_i \left[\beta^{-1} \log(\Lambda^3 c_i) - \mu_i \right] dV. \quad (2.9)$$

Now we have by (1.2) that for $|t| \ll 1$

$$\begin{aligned} & \frac{F_{\text{pot}}[c+td] - F_{\text{pot}}[c]}{t} \\ &= \frac{1}{2} \int_{\Omega} \frac{\rho(c+td)\psi(c+td) - \rho(c)\psi(c)}{t} dV + \frac{1}{2} \int_{\Gamma_N} \sigma \frac{\psi(c+td) - \psi(c)}{t} dS \\ &= \frac{1}{2} \int_{\Omega} \frac{\rho(c+td) - \rho(c)}{t} \psi(c+td) dV + \frac{1}{2} \int_{\Omega} \rho(c) \frac{\psi(c+td) - \psi(c)}{t} dV \\ & \quad + \frac{1}{2} \int_{\Gamma_N} \sigma \frac{\psi(c+td) - \psi(c)}{t} dS \quad (2.10) \\ &= \frac{1}{2} \sum_{i=1}^M \int_{\Omega} q_i d_i \psi(c+td) dV + \frac{1}{2} \int_{\Omega} \rho(c) \frac{\psi(c+td) - \psi(c)}{t} dV \\ & \quad + \frac{1}{2} \int_{\Gamma_N} \sigma \frac{\psi(c+td) - \psi(c)}{t} dS. \end{aligned}$$

By Lemma 2.2, we have

$$\frac{1}{2} \sum_{i=1}^M \int_{\Omega} q_i d_i \psi(c+td) dV \rightarrow \frac{1}{2} \sum_{i=1}^M \int_{\Omega} q_i d_i \psi(c) dV \quad \text{as } t \rightarrow 0. \quad (2.11)$$

For the remaining two terms in (2.10), we have by the weak formulation (2.2) for $\psi(c)$ and (2.4) for $\psi_D(c)$ with $\phi = [\psi(c+td) - \psi(c)]/t$ that

$$\begin{aligned}
 & \frac{1}{2} \int_{\Omega} \rho(c) \frac{\psi(c+td) - \psi(c)}{t} dV + \frac{1}{2} \int_{\Gamma_N} \sigma \frac{\psi(c+td) - \psi(c)}{t} dS \\
 &= \frac{1}{2} \int_{\Omega} \varepsilon \left(\bar{c} \right) \varepsilon_0 \nabla \psi(c) \cdot \nabla \left[\frac{\psi(c+td) - \psi(c)}{t} \right] dV \tag{2.12} \\
 &= \frac{1}{2} \int_{\Omega} \varepsilon \left(\bar{c} \right) \varepsilon_0 \nabla [\psi(c) - \psi_D(c)] \cdot \nabla \left[\frac{\psi(c+td) - \psi(c)}{t} \right] dV
 \end{aligned}$$

It now follows from the weak formulations for $\psi(c + td)$ and $\psi(c)$ (cf. (2.2)) with $\phi = \psi(c) - \psi_D(c)$, and Lemma 2.2 that

$$\begin{aligned}
 & \frac{1}{2} \int_{\Omega} \varepsilon \left(\bar{c} \right) \varepsilon_0 \nabla [\psi(c) - \psi_D(c)] \cdot \nabla \left[\frac{\psi(c+td) - \psi(c)}{t} \right] dV \\
 &= \frac{1}{2t} \int_{\Omega} \left[\varepsilon \left(\bar{c} \right) - \varepsilon \left(\bar{c} + t \bar{d} \right) \right] \varepsilon_0 \nabla [\psi(c) - \psi_D(c)] \cdot \nabla \psi(c+td) dV \\
 &+ \frac{1}{2t} \int_{\Omega} \varepsilon \left(\bar{c} + t \bar{d} \right) \varepsilon_0 \nabla [\psi(c) - \psi_D(c)] \cdot \nabla \psi(c+td) dV \\
 &- \frac{1}{2t} \int_{\Omega} \varepsilon \left(\bar{c} \right) \varepsilon_0 \nabla [\psi(c) - \psi_D(c)] \cdot \nabla \psi(c) dV \\
 &= -\frac{1}{2} \int_{\Omega} \frac{\varepsilon \left(\bar{c} + t \bar{d} \right) - \varepsilon \left(\bar{c} \right)}{t} \varepsilon_0 \nabla [\psi(c) - \psi_D(c)] \cdot \nabla \psi(c+td) dV \\
 &+ \frac{1}{2t} \int_{\Omega} \rho(c+td) [\psi(c) - \psi_D(c)] dV - \frac{1}{2t} \int_{\Omega} \rho(c) [\psi(c) - \psi_D(c)] dV \\
 &= -\frac{1}{2} \int_{\Omega} \left[\frac{\varepsilon \left(\bar{c} + t \bar{d} \right) - \varepsilon \left(\bar{c} \right)}{t} \varepsilon_0 - \sum_{i=1}^M d_i \varepsilon' \left(\bar{c} \right) \varepsilon_0 \right] \nabla [\psi(c) - \psi_D(c)] \cdot \nabla \psi(c+td) dV \\
 &- \frac{1}{2} \sum_{i=1}^M d_i \varepsilon' \left(\bar{c} \right) \varepsilon_0 \nabla [\psi(c) - \psi_D(c)] \cdot \nabla \psi(c+td) dV \\
 &+ \frac{1}{2} \sum_{i=1}^M \int_{\Omega} d_i q_i [\psi(c) - \psi_D(c)] dV \\
 &\rightarrow -\frac{1}{2} \sum_{i=1}^M \int_{\Omega} d_i \varepsilon' \left(\bar{c} \right) \varepsilon_0 \nabla [\psi(c) - \psi_D(c)] \cdot \nabla \psi(c) dV \\
 &+ \frac{1}{2} \sum_{i=1}^M \int_{\Omega} d_i q_i [\psi(c) - \psi_D(c)] dV \quad \text{as } t \rightarrow 0
 \end{aligned}$$

This and (2.10)–(2.12) lead to

$$\begin{aligned}
 \delta F_{\text{pot}} [c] [d] &= \lim_{t \rightarrow 0} \frac{F_{\text{pot}}[c+td] - F_{\text{pot}}[c]}{t} \\
 &= \sum_{i=1}^M \int_{\Omega} d_i q_i [\psi(c) - \frac{1}{2} \psi_D(c)] dV \tag{2.13} \\
 &- \frac{1}{2} \sum_{i=1}^M \int_{\Omega} d_i \varepsilon' \left(\bar{c} \right) \varepsilon_0 \nabla [\psi(c) - \psi_D(c)] \cdot \nabla \psi(c) dV
 \end{aligned}$$

We finally combine (2.9) and (2.13) to obtain the desired first variation.

2.2. Generalized Boltzmann distributions

We call $c = (c_1, \dots, c_M) \in X$ an equilibrium if the first variation $\delta F [c][d]$ defined by (2.5) exists and is equal to 0 for any $d \in L^\infty(\Omega, \mathbb{R}^M)$. If $c = (c_1, \dots, c_M) \in X$ satisfies the assumption in Theorem 2.1 and is an equilibrium, then $\delta_i F [c] = 0$ ($i = 1, \dots, M$) by Theorem 2.1. Straightforward calculations then lead to

$$c_i = c_i^\infty \exp \left\{ -\beta \left\{ q_i \left[\psi(c) - \frac{1}{2} \psi_D(c) \right] - \frac{1}{2} \varepsilon'(\bar{c}) \varepsilon_0 \nabla \psi(c) \cdot \nabla [\psi(c) - \psi_D(c)] \right\} \right\}, \quad (2.14)$$

where $c_i^\infty = \Lambda^{-3} e^{\beta \mu_i}$ ($1 \leq i \leq M$). We call these the generalized Boltzmann distributions, as they generalize the classical Boltzmann distributions $c_i = c_i^\infty e^{-\beta q_i \psi}$ ($i=1, \dots, M$) if ε does not depend on c , and $\psi_\infty = 0$ which implies $\psi_D = 0$. The effect of the boundary data was noted in [35, 36]. Note that in general $\varepsilon'(\bar{c}) \neq 0$ and hence (2.14) does not explicitly determine how the concentrations c_i ($i = 1, \dots, M$) depend on the potential ψ .

3. Second Variations

Let $a, b, c \in X$. We define

$$\delta^2 F[c][a, b] = \lim_{t \rightarrow 0} \frac{\delta F[c+ta][b] - \delta F[c][b]}{t},$$

if the quotient is defined when $|t| \ll 1$ and the limit exists, and call it the second variation of the free-energy functional F at c in the directions a and b .

For $c \in X$ and $a = (a_1, \dots, a_M) \in X$, let us denote by $\Psi(c, a)$ the unique weak solution to the boundary-value problem

$$\begin{cases} -\nabla \cdot \varepsilon(\bar{c}) \varepsilon_0 \nabla \Psi(c, a) = \sum_{i=1}^M a_i \left[q_i + \nabla \cdot \varepsilon'(\bar{c}) \varepsilon_0 \nabla \psi(c) \right] & \text{in } \Omega, \\ \varepsilon(\bar{c}) \varepsilon_0 \frac{\partial \Psi(c, a)}{\partial n} = \frac{\varepsilon'(\bar{c})}{\varepsilon(\bar{c})} \sigma & \text{on } \Gamma_N, \\ \Psi(c, a) = 0 & \text{on } \Gamma_D, \end{cases}$$

defined by $\Psi(c, a) \in H^1_{D,0}(\Omega)$ and

$$\int_{\Omega} \varepsilon(\bar{c}) \varepsilon_0 \nabla \Psi(c, a) \cdot \nabla \phi \, dV = \sum_{i=1}^M \int_{\Omega} a_i \left[q_i \phi - \varepsilon'(\bar{c}) \varepsilon_0 \nabla \psi(c) \cdot \nabla \phi \right] \, dV \quad \forall \phi \in H^1_{D,0}(\Omega). \quad (3.1)$$

Similarly, let us denote by $\Psi_D(c, a)$ the unique weak solution of the boundary-value problem

$$\begin{cases} -\nabla \cdot \varepsilon(\bar{c}) \varepsilon_0 \nabla \Psi_D(c, a) = \sum_{i=1}^M a_i \nabla \cdot \varepsilon'(\bar{c}) \varepsilon_0 \nabla \psi_D(c) & \text{in } \Omega, \\ \varepsilon(\bar{c}) \varepsilon_0 \frac{\partial \Psi_D(c, a)}{\partial n} = 0 & \text{on } \Gamma_N, \\ \Psi_D(c, a) = 0 & \text{on } \Gamma_D, \end{cases}$$

defined by $\Psi_D(c, a) \in H^1_{D,0}(\Psi)$ and

$$\int_{\Omega} \varepsilon(\bar{c}) \varepsilon_0 \nabla \Psi_D(c, a) \cdot \nabla \phi dV = - \sum_{i=1}^M \int_{\Omega} a_i \varepsilon'(\bar{c}) \varepsilon_0 \nabla \psi_D(c) \cdot \nabla \phi dV \quad \forall \phi \in H^1_{D,0}(\Omega). \quad (3.2)$$

The existence and uniqueness of each of these weak solutions is guaranteed by the Lax–Milgram Lemma. Note that $\Psi(c, a)$ and $\Psi_D(c, a)$ are linear in a .

Theorem 3.1

Let $\varepsilon \in C^2([0, \infty))$. Let $c = (c_1, \dots, c_M) \in X$. Assume there exist positive numbers δ_1 and δ_2 such that $\delta_1 < c_i(x) < \delta_2$ for a.e. $x \in \Omega$ and $i = 1, \dots, M$. Let $a = (a_1, \dots, a_M)$, $b = (b_1, \dots, b_M) \in L^\infty(\Omega, \mathbb{R}^M)$. We have

$$\begin{aligned} & \delta^2 F[c][a, b] \\ &= \int_{\Omega} \left\{ \varepsilon(\bar{c}) \varepsilon_0 \left[\nabla \Psi(c, b) \cdot \nabla \Psi_D(c, a) - \frac{1}{2} \nabla \Psi(c, a) \cdot \nabla \Psi(c, a) - \frac{1}{2} \nabla \Psi_D(c, a) \cdot \nabla \Psi(c, a) \right] \right. \\ & \left. - \frac{1}{2} \left(\sum_{i=1}^M b_i \right) \left(\sum_{j=1}^M a_j \right) \varepsilon''(\bar{c}) \varepsilon_0 \nabla \psi(c) \cdot \nabla [\psi(c) - \psi_{D(c)}] + \sum_{i=1}^M \frac{a_i b_i}{\beta c_i} dV \right\} \end{aligned}$$

Note that $\delta^2 F[c][a, b]$ is symmetric and bilinear in (a, b) . To prove this theorem, let us denote for $|t| \ll 1$

$$\Psi(c, a; t) = \frac{\psi(c+ta) - \psi(c)}{t} \quad \text{and} \quad \Psi_D(c, a; t) = \frac{\psi_D(c+ta) - \psi_D(c)}{t} \quad (3.3)$$

where $\psi(c+ta) \in H^1_D(\Omega)$ and $\psi_D(c+ta)$ are defined by (2.2) and (2.4), respectively, with c replaced by $c+ta$. We first prove the following:

Lemma 3.2

Under the assumption of Theorem 3.1, we have $\Psi(c, a; t) \rightarrow \Psi(c, a)$ and $\Psi_D(c, a; t) \rightarrow \Psi_D(c, a)$ in $H^1(\Omega)$ as $t \rightarrow 0$.

Proof—Consider $|t| \ll 1$. By the weak formulations for $\psi(c+ta)$ and $\psi(c)$ (cf. (2.2)) and the definition of $\rho(c+ta)$ and $\rho(c)$ (cf. (1.2)), we have for any $\phi \in H^1_D(\Omega)$ that

$$\int_{\Omega} \varepsilon(\bar{c} + t \bar{a}) \varepsilon_0 \nabla \psi(c+ta) \cdot \nabla \phi dV - \int_{\Omega} \varepsilon(\bar{c}) \varepsilon_0 \nabla \psi(c) \cdot \nabla \phi dV = t \sum_{i=1}^M \int_{\Omega} q_i a_i \phi dV.$$

With our notation $\Psi(c, a)$ and $\Psi(c, a; t)$, and the weak formulation for $\Psi(c, a)$ (cf. (3.1)), this leads to

$$\begin{aligned} & \int_{\Omega} \frac{\varepsilon(\bar{c}+t\bar{a})-\varepsilon(\bar{c})}{t} - \varepsilon_0 \nabla \psi(c+ta) \cdot \nabla \phi dV + \int_{\Omega} \varepsilon(\bar{c}) \nabla [\Psi(c, a; t) - \Psi(c, a)] \cdot \nabla \phi dV \\ &= \sum_{i=1}^M \int_{\Omega} a_i \varepsilon'(\bar{c}) \varepsilon_0 \nabla \psi(c) \cdot \nabla \phi dV. \end{aligned}$$

Setting $\phi = f_t := \Psi(c, a; t) - \Psi(c, a) \in H^1_{D,0}(\Omega)$, we then obtain

$$\begin{aligned} \int_{\Omega} \varepsilon(\bar{c}) \varepsilon_0 |\nabla f_t|^2 dV &= \sum_{i=1}^M \int_{\Omega} a_i \varepsilon'(\bar{c}) \varepsilon_0 \nabla \psi(c) \cdot \nabla f_t dV \\ &\quad - \int_{\Omega} \frac{\varepsilon(\bar{c}+t\bar{a})-\varepsilon(\bar{c})}{t} \varepsilon_0 \nabla \psi(c+ta) \cdot \nabla f_t dV \\ &= \sum_{i=1}^M \int_{\Omega} a_i \varepsilon'(\bar{c}) \varepsilon_0 [\nabla \psi(c) - \nabla \psi(c+ta)] \cdot \nabla f_t dV \\ &\quad + \int_{\Omega} \left[\sum_{i=1}^M a_i \varepsilon'(\bar{c}) - \frac{\varepsilon(\bar{c}+t\bar{a})-\varepsilon(\bar{c})}{t} \right] \varepsilon_0 \nabla \psi(c+ta) \cdot \nabla f_t dV. \end{aligned}$$

Since $\varepsilon'(\bar{c})$ is bounded in Ω and $\varepsilon(\bar{c}) \geq \varepsilon_{min}$ in Ω , we thus have by the assumption on $\varepsilon = \varepsilon(\bar{c})$, the Cauchy–Schwarz inequality, and Lemma 2.2 that

$$\begin{aligned} \varepsilon_{min} \varepsilon_0 \|\nabla f_t\|_{L^2(\Omega)} &\leq \left(\sum_{i=1}^M \|a_i\|_{L^\infty(\Omega)} \right) |\varepsilon'(0)| \varepsilon_0 \|\nabla \psi(c) - \nabla \psi(c+ta)\|_{L^2(\Omega)} \\ &\quad + \left\| \sum_{i=1}^M a_i \varepsilon'(\bar{c}) - \frac{\varepsilon(\bar{c}+t\bar{a})-\varepsilon(\bar{c})}{t} \right\|_{L^\infty(\Omega)} \varepsilon_0 \|\nabla \psi(c+ta)\|_{L^2(\Omega)} \\ &\rightarrow 0 \quad \text{as } t \rightarrow 0. \end{aligned}$$

This and the Poincaré inequality for functions in $H^1_{D,0}(\Omega)$ imply the convergence $\Psi(c, a; t) \rightarrow \Psi(c, a)$ in $H^1(\Omega)$ as $t \rightarrow 0$. The convergence $\Psi_D(c, a; t) \rightarrow \Psi_D(c, a)$ in $H^1(\Omega)$ as $t \rightarrow 0$ can be proved similarly.

Proof—[Proof of Theorem 3.1] We first consider $F_{ent}[c]$ defined in (2.8). By the boundedness of all a , b , and c , and Lebesgue’s Dominated Convergence Theorem, we have by (2.9) that

$$\begin{aligned}
 \delta^2 F_{\text{ent}} [c] [a, b] : &= \lim_{t \rightarrow 0} \frac{\delta F_{\text{ent}} [c+ta] [b] - \delta F_{\text{ent}} [c] [b]}{t} \\
 &= \lim_{t \rightarrow 0} \sum_{i=1}^M \int_{\Omega} b_i \frac{\beta^{-1} \log(\Lambda^3(c_i+ta_i)) - \beta^{-1} \log(\Lambda^3 c_i)}{t} dV \\
 &= \sum_{i=1}^M \int_{\Omega} b_i \beta^{-1} \frac{d}{dt} \log(c_i+ta_i) \Big|_{t=0} dV \\
 &= \sum_{i=1}^M \int_{\Omega} \frac{a_i b_i}{\beta c_i} dV.
 \end{aligned} \tag{3.4}$$

We now consider $F_{\text{pot}}[c]$ defined in (2.7). By (2.13) and using our notation $\Psi(c, a; t)$ and $\Psi_D(c, a; t)$ (cf. (3.3)), we have

$$\begin{aligned}
 &\frac{1}{t} \{ \delta F_{\text{pot}} [c+ta] [b] - \delta F_{\text{pot}} [c] [b] \} \\
 &= \sum_{i=1}^M \int_{\Omega} b_i q_i \Psi (c, a; t) dV - \frac{1}{2} \sum_{i=1}^M \int_{\Omega} b_i q_i \Psi_D (c, a; t) dV \\
 &\quad - \frac{1}{2} \sum_{i=1}^M \int_{\Omega} b_i \left[\frac{\varepsilon' (\bar{c} + t \bar{a} - \varepsilon' (\bar{c}))}{t} \right] \varepsilon_0 \nabla \psi (c+ta) \cdot \nabla [\psi (c+ta) - \psi_D (c+ta)] dV \\
 &\quad - \frac{1}{2} \sum_{i=1}^M \int_{\Omega} b_i \varepsilon' (\bar{c}) \varepsilon_0 \nabla \psi (c+ta) \cdot \nabla [\Psi (c, a; t) - \Psi_D (c, a; t)] dV \\
 &\quad - \frac{1}{2} \sum_{i=1}^M \int_{\Omega} b_i \varepsilon' (\bar{c}) \varepsilon_0 \nabla \Psi (c, a, ; t) \cdot \nabla [\psi (c) - \psi_D (c)] dV.
 \end{aligned}$$

Consequently, since

$$\frac{\varepsilon' (\bar{c} + t \bar{a} - \varepsilon' (\bar{c}))}{t} \rightarrow \sum_{j=1}^M a_j \varepsilon'' (\bar{c}) \quad \text{in } L^\infty (\Omega),$$

we have by Lemma 2.2 and Lemma 3.2, and by rearranging terms, that

$$\begin{aligned}
 \delta^2 F_{\text{pot}} [c] [a, b] : &= \lim_{t \rightarrow 0} \frac{1}{t} \{ \delta F_{\text{pot}} [c+ta] [b] - \delta F_{\text{pot}} [a] [b] \} \\
 &= \sum_{i=1}^M \int_{\Omega} b_i q_i \Psi (c, a) dV - \frac{1}{2} \sum_{i=1}^M \int_{\Omega} b_i q_i \Psi_D (c, a) dV \\
 &\quad - \frac{1}{2} \int_{\Omega} \left(\sum_{i=1}^M b_i \right) \left(\sum_{j=1}^M a_j \right) \varepsilon'' (\bar{c}) \varepsilon_0 \nabla \psi (c) \cdot \nabla [\psi (c) - \psi_D (c)] dV \\
 &\quad - \frac{1}{2} \sum_{i=1}^M \int_{\Omega} b_i \varepsilon' (\bar{c}) \varepsilon_0 \nabla \psi (c) \cdot [\nabla \Psi (c, a) - \nabla \Psi_D (c, a)] dV \\
 &\quad - \frac{1}{2} \sum_{i=1}^M \int_{\Omega} b_i \varepsilon' (\bar{c}) \varepsilon_0 \nabla \Psi (c, a) \cdot \nabla [\psi (c) - \psi_D (c)] dV \\
 &= - \frac{1}{2} \int_{\Omega} \left(\sum_{i=1}^M b_i \right) \left(\sum_{j=1}^M a_j \right) \varepsilon'' (\bar{c}) \varepsilon_0 \nabla \psi (c) \cdot \nabla [\psi (c) - \psi_D (c)] dV \\
 &\quad + \sum_{i=1}^M \int_{\Omega} b_i q_i \Psi (c, a) dV - \frac{1}{2} \sum_{i=1}^M \int_{\Omega} b_i q_i \Psi_D (c, a) dV \\
 &\quad - \sum_{i=1}^M \int_{\Omega} b_i \varepsilon' (\bar{c}) \varepsilon_0 \nabla \psi (c) \cdot \Psi (c, a) dV \\
 &\quad + \frac{1}{2} \sum_{i=1}^M \int_{\Omega} b_i \varepsilon' (\bar{c}) \varepsilon_0 \nabla \psi (c) \cdot \Psi_D (c, a) dV \\
 &\quad + \frac{1}{2} \sum_{i=1}^M \int_{\Omega} b_i \varepsilon' (\bar{c}) \varepsilon_0 \nabla \psi_D (c) \cdot \Psi (c, a) dV \\
 &= - \frac{1}{2} \int_{\Omega} \left(\sum_{i=1}^M b_i \right) \left(\sum_{j=1}^M a_j \right) \varepsilon'' (\bar{c}) \varepsilon_0 \nabla \psi (c) \cdot \nabla [\psi (c) - \psi_D (c)] dV \\
 &\quad + \sum_{i=1}^M \int_{\Omega} b_i \left[q_i \Psi (c, a) - \varepsilon' (\bar{c}) \varepsilon_0 \nabla \psi (c) \cdot \nabla \Psi_D (c, a) \right] dV \\
 &\quad - \frac{1}{2} \sum_{i=1}^M \int_{\Omega} b_i \left[q_i \Psi_D (c, a) - \varepsilon' (\bar{c}) \varepsilon_0 \nabla \psi (c) \cdot \nabla \Psi_D (c, a) \right] dV \\
 &\quad + \frac{1}{2} \sum_{i=1}^M \int_{\Omega} b_i \varepsilon' (\bar{c}) \varepsilon_0 \nabla \psi_D (c) \cdot \nabla \Psi (c, a) dV.
 \end{aligned}$$

By the weak formulation for $\Psi(c, b)$ (cf. (3.1) with b replacing a) with $\phi = \Psi(c, a)$, the weak formulation for $\Psi(c, b)$ (cf. (3.1) with b replacing a) with $\phi = \Psi_D(c, a)$, and the weak formulation for $\Psi_D(c, b)$ (cf. (3.2) with b replacing a) with $\phi = \Psi(c, a)$, we therefore obtain

$$\begin{aligned}
 \delta^2 F_{\text{pot}} [a] [a, b] &- \frac{1}{2} \int_{\Omega} \left(\sum_{i=1}^M b_i \right) \left(\sum_{j=1}^M a_j \right) \varepsilon'' (\bar{c}) \varepsilon_0 \nabla \psi (c) \cdot \nabla [\psi (c) - \psi_D (c)] dV \\
 &+ \int_{\Omega} \varepsilon (\bar{c}) \varepsilon_0 \nabla \Psi (c, a) \cdot \nabla \Psi (c, a) dV \\
 &- \frac{1}{2} \int_{\Omega} \varepsilon (\bar{c}) \varepsilon_0 \nabla \Psi (c, a) \cdot \nabla \Psi_D (c, a) dV \\
 &- \frac{1}{2} \int_{\Omega} \varepsilon (\bar{c}) \varepsilon_0 \nabla \Psi_D (c, a) \cdot \nabla \Psi (c, a) dV
 \end{aligned}$$

This and (3.4) imply the desired second variation.

4. Non-Convexity of the Free-Energy Functional

By Theorem 3.1, the second variation $\delta^2 F [c]$ is not necessarily positive definite, i.e., $\delta^2 F [c]$ may not be positive, as $\varepsilon''(\bar{c}) \geq 0$ by our assumption that is based on experimental data. This indicates that the free-energy functional (1.1) may be nonconvex. We investigate this non-convexity by examining the generalized Boltzmann distributions. If we assume $\psi_\infty = 0$ on Γ_D , then $\psi_D = 0$ in Ω , cf. (2.4), and hence the generalized Boltzmann distributions (2.14) become

$$c_i = c_i^\infty e^{-\beta q_i \psi} e^{\beta \varepsilon'(\bar{c}) \varepsilon_0 |\nabla \psi|^2 / 2}, \quad i=1, \dots, M, \quad (4.1)$$

where $\psi = \psi(c)$. Summing over all i and using the notation $\bar{c} = \sum_{i=1}^M c_i$, we obtain

$$\bar{c} = \left(\sum_{i=1}^M c_i^\infty e^{-\beta q_i \psi} \right) e^{\beta \varepsilon'(\bar{c}) \varepsilon_0 |\nabla \psi|^2 / 2},$$

Based on these considerations, we define for any given $s \in \mathbb{R}$ and $v \geq 0$

$$G(\bar{c}) = G_{s,v}(\bar{c}) = \left(\sum_{i=1}^M c_i^\infty e^{-\beta q_i s} \right) e^{\beta \varepsilon'(\bar{c}) \varepsilon_0 v^2 / 2} - \bar{c} \quad \forall \bar{c} \geq 0.$$

Notice that if $c = (c_1, \dots, c_M)$ satisfies the generalized Boltzmann distributions (4.1), $s = \psi(c)$, and $v = |\nabla \psi(c)|$, then $G(\bar{c}) = 0$ with $\bar{c} = \sum_{i=1}^M c_i$.

We now consider an ionic solution occupying the annulus region $10 < r = |x| < 60$ (in Å) with the charge density $\sigma = -0.02 \text{ e}/\text{Å}^2$ on $r = 10$. We assume there are two ionic species in the solution with $Z_1 = 1, Z_2 = -1, c_1^\infty = 0.1 \text{ M}$, and $c_2^\infty = 0.1 \text{ M}$. We choose

$\varepsilon(\bar{c}) = 70 e^{-0.22 \bar{c}} + 10$ which we used to fit experimental data, cf. Figure 1.1. From our numerical computational results (cf. Section 5 for details), we fix a few selected values of ψ and $|\nabla \psi|$ near the charged surface $r = 10$, and then plot in Figure 4.1 (Left) the graph of

function $G(\bar{c}) = G_{s,v}(\bar{c}) = G_{\psi, |\nabla \psi|}(\bar{c})$, where we use c instead of \bar{c} instead of ψ . We observe that there are multiple solutions to the equation $G(c) = 0$ for some values of ϕ and $|\nabla \phi|$, indicating that the generalized Boltzmann distributions may not determine uniquely the concentrations through the electrostatic potential. In Figure 4.1 (Right), we plot zeros of $G(c) = 0$ vs. c . We see that there are three zeros when the electrostatic potential is large in magnitude.

We now construct two examples to show that the free-energy functional (1.1) is in general nonconvex. For simplicity, we take ε_0 to be the unity.

Example 1

Let $\sigma, \beta, \lambda, \mu \in \mathbb{R}$ with $\beta > 0$ and $\lambda > 0$. We consider the functional

$$F [c] = \int_0^1 \frac{1}{2} c \psi dx + \frac{1}{2} \sigma \psi (0) + \int_1^0 [\beta^{-1} c \log (\lambda c) - \mu c] dx \quad (4.2)$$

for functions $c = c(x) \geq 0$ with $x \in (0,1)$, where the potential $\psi = \psi(x)$ is determined by

$$\begin{cases} (\varepsilon (c(x) \psi'(x)))' = -c(x), & x \in (0,1) . \\ \psi(1) = 0, \\ \varepsilon (c(0) \psi') = -\sigma, \end{cases}$$

Here, $\varepsilon(c) = 70e^{-0.22c} + 10$, which was used to fit experimental data in Figure 1.1. This model can be viewed as reduced from a three-dimensional model with the ionic concentration and electrostatic potential only varying in the x -coordinate direction.

If c is a constant function, then we have by simple calculations that

$$\begin{aligned} \psi(x) &= -\frac{cx^2}{2\varepsilon(c)} - \frac{\sigma x}{\varepsilon(c)} + \frac{c}{2\varepsilon(c)} + \frac{\sigma}{\varepsilon(c)}, & x \in (0,1) \\ F[c] &= \frac{c^2 + 3c\sigma + 3\sigma^2}{6\varepsilon(c)} + \beta^{-1} c \log \left(\frac{c}{c^\infty} \right), & c > 0, \end{aligned} \quad (4.3)$$

where $c^\infty = \lambda^{-1} e^{\beta\mu}$. The function $F [c]$, with $\sigma = -0.04$, $\beta^{-1} = 1$, and $c^\infty = 0.1$, is plotted in Figure 4.2. We find that it has two local minima at $c = 0$ and $c \approx 48.4$, and that it is nonconvex. Hence, the functional $F [c]$ defined in (4.2) is not convex in general.

Example 2

We consider the free-energy functional

$$F [c] = \int_0^1 \left(\frac{1}{2} c \psi + c \log c - 2c \right) dx \quad (4.4)$$

for functions $c = c(x) \geq 0$ with $x \in (0,1)$, where the potential $\psi = \psi(x)$ is determined by

$$\begin{cases} (\varepsilon (c(x) \psi'(x)))' = -c(x), & x \in (0,1) . \\ \psi(0) = \psi(1) = 0, \end{cases}$$

The function $\varepsilon = \varepsilon(c)$ is defined by

$$\varepsilon(c) = \begin{cases} \frac{1025}{36} - \frac{50}{9}c & \text{if } 0 \leq c < 4, \\ \frac{25}{18}(c-6)^2 + \frac{25}{36} & \text{if } 4 \leq c < 6, \\ \frac{25}{36} & \text{if } 6 \leq c < \infty. \end{cases} \quad (4.5)$$

It can be verified that this is a C^1 -function, monotonically decreasing, convex, and bounded above and below by positive constants. See Figure 4.3 (Left) for a plot of this function.

For constant functions c , we have

$$\begin{aligned} \psi(x) &= -\frac{cx^2}{2\varepsilon(c)} + \frac{cx}{2\varepsilon(c)}, \quad x \in (0, 1), \\ F[c] &= \frac{c^2}{24\varepsilon(c)} + c \log(c) - 2c, \quad c > 0. \end{aligned} \quad (4.6)$$

Figure 4.3 (Right) is a plot of the function $F[c]$ defined in (4.6). We see clearly that this function $F[c]$ is not convex. Hence the functional $F[c]$ defined in (4.4) is not convex.

5. Numerical Study of a Model System

We minimize numerically the free-energy functional (1.1) and (1.3) with

$$\Omega = \{x \in \mathbb{R}^3 : R_N < |x| < R_D\}, \quad \Gamma_N = \{x \in \mathbb{R}^3 : |x| = R_N\}, \quad \Gamma_D = \{x \in \mathbb{R}^3 : |x| = R_D\},$$

where R_D and R_N are two given positive numbers such that $R_D < R_N$. We assume that $\rho_f = \rho_f(r)$ is a function of $r = |x|$, ψ_∞ is a constant, and σ is also a constant. By the radial symmetry, we assume the concentrations and potential are functions of $r = |x|$ and write $c = c(r)$ and $\psi = \psi(r)$. The free-energy functional (1.1) and the boundary-value problem of Poisson's equation (1.3) become now

$$F[c] = 4\pi \int_{R_N}^{R_D} \left\{ \frac{1}{2} \left(\rho_f + \sum_{i=1}^M q_i c_i \right) \psi + \sum_{i=1}^M \beta^{-1} c_i \left[\log \left(\frac{c_i}{c_i^\infty} \right) - 1 \right] \right\} r^2 dr + 2\pi\sigma R_N^\psi(R_N), \quad (5.1)$$

$$\begin{cases} \varepsilon(\bar{c}) \psi''(r) + \varepsilon'(\bar{c}) \bar{c}'(r) \psi'(r) + \frac{2}{r} \varepsilon(\bar{c}) \psi'(r) = -\frac{1}{\varepsilon_0} \left[\rho_f + \sum_{i=1}^M q_i c_i(r) \right] & \text{if } R_N < r < R_D, \\ -\varepsilon(c(R_N)) \varepsilon_0 \psi'(R_N) = \sigma, \\ \psi(R_D) = \psi_\infty. \end{cases} \quad (5.2)$$

Here we use c_i^∞ instead of μ_i ($i = 1, \dots, M$) as input parameters. We have $\mu_i \beta^{-1} \log(\Lambda^3 c_i^\infty)$ ($i = 1, \dots, M$). With our radially symmetric setting, we can easily observe and verify that the solution ψ_D to the boundary-value problem (2.3) is $\psi_D = \psi_\infty$, a constant. By Theorem 2.1, the first variations of the free-energy functional (5.1) in the coordinate directions are then given by

$$\delta_i F [c] (r) = q_i \left[\psi (r) - \frac{1}{2} \psi_\infty \right] - \frac{1}{2} \varepsilon' \left(\bar{c} (r) \right) \varepsilon_0 \psi' (r) \left[\psi' (r) - \psi_\infty \right] + \beta^{-1} \log \left(\frac{c_i (r)}{c_i^\infty} \right), \quad R_N < r < R_D, i=1, \dots, M. \tag{5.3}$$

We employ a steepest descent method to minimize the free-energy functional (5.1). After initializing the concentrations $c = (c_1, \dots, c_M)$, we follow these steps:

- (1) Solve Poisson’s equation (5.2) to update the potential ψ .
- (2) Compute the first variations $\delta_i F [c] (i = 1, \dots, M)$ by (5.3).
- (3) Update the concentrations: $c_i \leftarrow c_i - \gamma d_i (i = 1, \dots, M)$, where $\gamma > 0$ is a pre-chosen parameter.
- (4) Check if $\max_{1 \leq i \leq M} \|\delta_i F [c]\|_{L^\infty} (R_N, R_D) < \varepsilon_{tol}$ with a pre-chosen tolerance ε_{tol} . If not, go back to (1).

We choose the parameter γ in Step (3) to be very small to ensure that all $c_i > 0$ in each iteration. In case $c_i < 0$ for some i , we can change γ to a smaller value to update c_i . Note that we only find numerically local minimizers that are sometimes more interesting in terms of physical properties than global minimizers.

We now fix $R_N = 10 \text{ \AA}$ and $R_D = 60 \text{ \AA}$, and vary the surface charge density σ from -0.005 to -0.025 e/\AA^2 . As surface charges generally represent the main part of fixed charges, we set $\rho_f = 0$. Moreover, since we are mainly interested in the counterion concentrations and electrostatic potentials near the charged surface, we set $\psi_\infty = 0$. We use $k_B T$ as units of energy. We consider two systems.

System I: $M = 2, Z_1 = 1, Z_2 = -1, c_1^\infty = 0.1 \text{ M}$, and $c_2^\infty = 0.1 \text{ M}$.

System II: $M = 3, Z_1 = 2, Z_2 = 1, Z_3 = -2, c_1^\infty = 0.1 \text{ M}, c_2^\infty = 0.1 \text{ M}, c_3^\infty = 0.1 \text{ M}$.

In each of our numerical computations, we observe the decay of the free energy and the convergence of concentrations in our iterations. This indicates that our numerical method is reliable.

5.1. Comparison of different dielectric relations: Counterion depletion

We compare equilibrium concentrations and electrostatic potentials corresponding to the

following four different dielectric coefficient functions $\varepsilon = \varepsilon_i \left(\bar{c} \right) : \left(\bar{c} \geq 0 \right)$:

$$\varepsilon_1 \left(\bar{c} \right) = 80; \quad \varepsilon_2 \left(\bar{c} \right) = 80 - 20 \bar{c}; \quad \varepsilon_3 \left(\bar{c} \right) = \frac{80}{1 + 0.25 \bar{c}}; \quad \varepsilon_4 \left(\bar{c} \right) = 70 e^{-0.22 \bar{c}} + 10. \tag{5.4}$$

Note that all these functions are convex and monotonically decreasing with the maximum value 80 at $\bar{c} = 0$. In addition $\varepsilon_3(\infty) = 0$ and $\varepsilon_4(\infty) = 10$. The linear dependence $\varepsilon_2 \left(\bar{c} \right)$ is

used in [7]. The form $\varepsilon_3\left(\bar{c}\right)$ is proposed in [31]. We used $\varepsilon_4\left(\bar{c}\right)$ to fit the experiment data in Figure 1.1.

We consider System I with the surface charge density $\sigma = -0.005 \text{ e}/\text{\AA}^2$. In Figure 5.1, we plot profiles of the equilibrium concentrations for both counterion and coion species for the four different dielectric coefficient defined in (5.4). The four concentration profiles for the species of coions nearly overlap and become one. It is the curve below all the other four for

the counterion concentrations. The inset shows the graph of $\varepsilon_i\left(\bar{c}(r)\right)$ ($1 \leq i \leq 4$) ($1 \leq i \leq 4$) as a function of the radial variable r . We observe differences of the counterion concentrations in the vicinity of the charged surface, even at such a relatively low surface

charge density. The counterion concentrations corresponding to $\varepsilon_2\left(\bar{c}\right)$, $\varepsilon_3\left(\bar{c}\right)$, and $\varepsilon_4\left(\bar{c}\right)$ are smaller than that predicted by the classical PB theory that corresponds to $\varepsilon_1\left(\bar{c}\right)$. Such counterion depletion is expected as explained in Introduction and as found in [7].

We now still consider System I but increase the surface charge density to $\sigma = -0.012 \text{ e}/\text{\AA}^2$. In Figure 5.2, we plot concentrations and potential similar to those in Figure 5.1. We see clearly that the counterion depletion near the charged surface is enhanced for the

concentration-dependent dielectric coefficient $\varepsilon = \varepsilon_i\left(\bar{c}\right)$ ($i = 2, 3, 4$). This is because that the increase of the surface charge leads to the increase of the electric field, which in turn

decreases more the concentration by the factor $e^{\beta \varepsilon'(\bar{c}) \varepsilon_0 |\nabla \psi|^2 / 2}$ in the generalized

Boltzmann distributions, since $\varepsilon'(\bar{c}) < 0$ is larger. We find that, for the case of linear

dependence $\varepsilon = \varepsilon_2\left(\bar{c}\right)$, our numerical solution is quite sensitive. As the concentration becomes large, the dielectric coefficient can be very close to zero and even negative, leading to an unphysical situation that corresponds to the loss of ellipticity mathematically.

5.2. Effect of surface charges and bulk concentrations: Non-monotonicity of counterion concentrations

We now consider System I with $\varepsilon = \varepsilon_4\left(\bar{c}\right)$ defined in (5.4). We compute the equilibrium concentration and electrostatic potential with the surface charge densities $\sigma = -0.01 \text{ e}/\text{\AA}^2$, $-0.015 \text{ e}/\text{\AA}^2$, $-0.02 \text{ e}/\text{\AA}^2$, and $-0.025 \text{ e}/\text{\AA}^2$, respectively, and plot our numerical results in Figure 5.3. We observe that the counterion concentration is non-monotonic for a large

surface charge density. The dielectric function $\varepsilon_i\left(\bar{c}(r)\right)$ is also non-monotonic. Moreover, for large surface charge densities, as the surface charge increases, the counterion concentration at the surface (i.e., at $r = R_N = 10 \text{ \AA}$) decreases, and the peak of the counterion concentration profile gets higher and moves further away from the surface. All these result

from the competition between the surface-counterion attraction and the counterion depletion near the surface.

In Figure 5.4, we plot the counterion concentration at the charged surface and the maximum value of counterion concentration as functions of the surface charge density. For comparison, we also plot the results predicted by the classical PB theory. We observe that the differences are significant for large surface charges: the counterion concentration at the charged surface predicted using $\varepsilon=\varepsilon_4\left(\bar{c}\right)$ decreases but that predicted by the classical PB equation increases. Moreover, the maximum value of counterion concentration predicted with $\varepsilon=\varepsilon_2\left(\bar{c}\right)$ increases as the surface charge density increases. We also plot the electrostatic potential at the charged surface in Figure 5.4 (Right). As the surface charge density increases, the electrostatic potentials at the charged surface predicted by the classical PB are weaker than those predicted with $\varepsilon=\varepsilon_4\left(\bar{c}\right)$. This is because that the screening effect with the ionic decrement is weaker.

We now fix the surface charge density $\sigma = -0.012 \text{ e}/\text{\AA}^2$ and vary the bulk concentrations c_i^∞ ($i = 1, 2$). From Figure 5.5 (Left), we observe that larger bulk concentrations lead to the stronger depletion effect. From Figure 5.5 (Right), we see that the counterion distribution is monotonic for low bulk concentrations and is non-monotonic after bulk concentrations exceed 0.2 M. Their differences increase as the bulk concentrations increase.

We now consider System II in which there are two species of counterions and one species of coions. In Figure 5.6, we plot concentration profiles for different values of surface charge density. We can again observe the ionic depletion for high surface charges.

6. Conclusions

We have studied a variational problem of minimizing a mean-field electrostatic free-energy functional to investigate how the ionic concentration dependent dielectric response can affect the equilibrium properties of electrostatic interactions of an ionic solution near a charged surface. Our basic modeling assumption is that the dependence of the dielectric coefficient on the sum of individual ionic concentrations is qualitatively the same as that on the salt concentrations for which experimental data are available. Such dependence is expressed mathematically as a continuous, monotonically decreasing, and convex function.

We have rigorously derived the first and second variations of the free-energy functional. Analytic formulas of such variations are useful in understanding the behavior of such a functional and in numerical computations. From the generalized Boltzmann distributions, we see that the ionic depletion can occur due to the high concentration low permittivity relation. The formula of the second variation of the functional indicates the functional can be nonconvex. We indeed show that it is so for some model systems.

We have also developed a numerical method and performed computations with a three-dimensional, radially symmetric geometry for a system with a single counterion species or a

system with two multi-valence counterion species. Our computational results show the ionic depletion near a charged surface with both low and high surface charges. Moreover, we have demonstrated that the increase of the surface charge density will lead to the non-monotonicity of concentration profiles. These results confirm experimental findings and also indicate that the classical PB theory does not capture the ionic depletion and other properties. One of the key points is that the counterions are attracted to the charged surface but in the meantime crowded counterions decreases the permittivity of the solution. With our efficient mean-field variational model, we have confirmed this.

It should be noted that a linear dependence $\varepsilon = \varepsilon_2 \left(\frac{\bar{c}}{c} \right)$ (cf. (5.4)) leads to the illposedness of Poisson's equation (cf. (1.3)). The nonlinear dependence of the dielectric coefficient on the ionic concentrations, however, leads to the lack of compactness needed in proving the existence of a minimizer by the usual argument of direct methods in the calculus of variations. To prove the existence, we will then need to construct carefully a free-energy-minimizing sequence that is weakly compact. The nonconvexity of the functional is different from that for the classical PB functional. It will be interesting to understand if such nonconvexity can be used to model the transition from weak to strong interactions in an ionic solution.

Our numerical algorithm is fairly general. The key of our algorithm is the self-consistency: In each step of relaxing the free-energy functional, we solve Poisson's equation with the concentration dependent dielectric coefficient. We update the concentrations and electrostatic potential alternatively. If one simply uses the classical Boltzmann distributions for c_i 's in $\varepsilon = \varepsilon \left(\frac{\bar{c}}{c} \right)$, one may not be able to capture the ionic depletion as shown in the recent work [38].

One of the ion-specific properties is the ionic size effect. In recent years, the PB-like mean-field models that account for ionic size effects have been developed [5, 7, 8, 22, 35–37, 39, 55, 59, 61]. Our experience is that a large (in terms of magnitude) surface charge density is needed to capture the ionic size effect in such models, while only a small charge density is needed to capture the ionic decrement near a charged surface. It will be therefore interesting to see the transition characterized by the surface charge density. Another important issue that we have not addressed here is the Born solvation energy of ions [41, 56, 60]. Additional equations may be needed to describe such energy. It is interesting to understand whether the inclusion of the Born solvation energy will also lead to the correction term in the generalized Boltzmann distributions. Finally, in terms of applications, how to apply our results to modeling charged macromolecules, such as proteins, in an aqueous environment is of great interest.

Acknowledgments

The authors thank Dr. Joachim Dzubiella, Dr. Zhenli Xu, Dr. Zhongming Wang, and Dr. Yanxiang Zhao for many helpful discussions. The authors also thank the anonymous referees for their helpful comments and suggestions.

REFERENCES

- [1]. Abrashkin A, Andelman D, Orland H. Dipolar Poisson–Boltzmann equation: Ions and dipoles close to charge interfaces. *Phys. Rev. Lett.* 2007; 99:077801. [PubMed: 17930925]
- [2]. Adams, R. *Sobolev Spaces*. Academic Press; New York: 1975.
- [3]. Andelman, D. Electrostatic properties of membranes: The Poisson–Boltzmann theory. Lipowsky, R.; Sackmann, E., editors. Vol. 1. *Handbook of Biological Physics*; Elsevier: 1995. p. 603–642.
- [4]. Andelman, D. Introduction to electrostatics in soft and biological matter. In: Poon, W.; Andelman, D., editors. *Proceedings of the Nato ASI & SUSSP on “Soft condensed matter physics in molecular and cell biology”* (2005). Taylor & Francis; New York: 2006. p. 97–122.
- [5]. Ben-Yaakov D, Andelman D, Harries D, Podgornik R. Beyond standard Poisson–Boltzmann theory: Ion-specific interactions in aqueous solutions. *J. Phys.: Condens. Matter.* 2009; 21:424106. [PubMed: 21715841]
- [6]. Ben-Yaakov D, Andelman D, Harries D, Podgornik R. Ions in mixed dielectric solvents: Density profiles and osmotic pressure between charged interfaces. *J. Phys. Chem. B.* 2009; 113:6001–6011. [PubMed: 19338312]
- [7]. Ben-Yaakov D, Andelman D, Podgornik R. Dielectric decrement as a source of ion-specific effects. *J. Chem. Phys.* 2011; 134:074705. [PubMed: 21341867]
- [8]. Borukhov I, Andelman D, Orland H. Steric effects in electrolytes: A modified Poisson–Boltzmann equation. *Phys. Rev. Lett.* 1997; 79:435–438.
- [9]. Buchner R, Hefter GT, Barthel J. Dielectric relaxation of aqueous NaF and KF solutions. *J. Chem. Soc. Faraday Trans.* 1994; 90:2475–2479.
- [10]. Buchner R, Hefter GT, May PM. Dielectric relaxation of aqueous NaCl solutions. *J. Phys. Chem. A.* 1999; 103:1–9.
- [11]. Chapman DL. A contribution to the theory of electrocapillarity. *Philos. Mag.* 1913; 25:475–481.
- [12]. Che J, Dzubiella J, Li B, McCammon JA. Electrostatic free energy and its variations in implicit solvent models. *J. Phys. Chem. B.* 2008; 112:3058–3069. [PubMed: 18275182]
- [13]. Davis ME, McCammon JA. Electrostatics in biomolecular structure and dynamics. *Chem. Rev.* 1990; 90:509–521.
- [14]. Debye P, Hückel E. Zur Theorie der Elektrolyte. *Physik. Zeitschr.* 1923; 24:185–206.
- [15]. Démary V, Dean DS, Podgornik R. Electrostatic interactions mediated by polarizable counterions: Weak and strong coupling limits. *J. Chem. Phys.* 2012; 137:174903. [PubMed: 23145746]
- [16]. Dill KA. Dominant forces in protein folding. *Biochemistry.* 1990; 29:7133–7155. [PubMed: 2207096]
- [17]. Drude P, Nernst W. Über Elektrostriktion durch freie Ionen. *Z. Phys. Chem.* 1984; 15:79–85.
- [18]. Evans LC. *Partial Differential Equations*, volume 19 of *Graduate Studies in Mathematics*. Amer. Math. Soc (2nd). 2010
- [19]. Fixman F. The Poisson–Boltzmann equation and its application to polyelectrolytes. *J. Chem. Phys.* 1979; 70:4995–5005.
- [20]. Fogolari F, Briggs JM. On the variational approach to Poisson–Boltzmann free energies. *Chem. Phys. Lett.* 1997; 281:135–139.
- [21]. Fogolari F, Brigo A, Molinari H. The Poisson–Boltzmann equation for biomolecular electrostatics: a tool for structural biology. *J. Mol. Recognit.* 2002; 15:377–392. [PubMed: 12501158]
- [22]. Frydel D. Polarizable Poisson–Boltzmann equation: The study of polarizability effects on the structure of a double layer. *J. Chem. Phys.* 2011; 134:234704. [PubMed: 21702573]
- [23]. Gilbarg, D.; Trudinger, NS. *Elliptic Partial Differential Equations of Second Order*. 2nd. Springer-Verlag; 1998.
- [24]. Gouy M. Sur la constitution de la charge électrique a la surface d’un électrolyte. *J. Phys. Théor. Appl.* 1910; 9:457–468.

- [25]. Grochowski P, Trylska J. Continuum molecular electrostatics, salt effects and counterion binding —A review of the Poisson–Boltzmann model and its modifications. *Biopolymers*. 2008; 89:93–113. [PubMed: 17969016]
- [26]. Hasted, JB. *Aqueous Dielectrics*. Chapman and Hall; London: 1973.
- [27]. Hasted JB, Riston M, Collie CH. Dielectric properties of aqueous ionic solutions. Parts I and II. *J. Chem. Phys.* 1948; 16:1–21.
- [28]. Hille, B. *Ion Channels of Excitable Membranes*. 3rd. Sinauer Associates; 2001.
- [29]. Honig B, Nicholls A. Classical electrostatics in biology and chemistry. *Science*. 1995; 268:1144–1149. [PubMed: 7761829]
- [30]. Jackson, JD. *Classical Electrodynamics*. 3rd. Wiley; New York: 1999.
- [31]. Kalcher I, Dzubiella J. Structure-thermodynamics relation of electrolyte solutions. *J. Chem. Phys.* 2009; 130:134507. [PubMed: 19355751]
- [32]. Landau, LD.; Lifshitz, EM.; Pitaevski, LP. *Electrodynamics of Continuous Media*. 2nd. Butterworth–Heinemann; 1993.
- [33]. Lattey RT. The dielectric constants of electrolytic solutions. *Philos. Mag.* 1921; 41:829–848.
- [34]. Levy A, Andelman D, Orland H. Dielectric constant of ionic solutions: A field-theory approach. *Phys. Rev. Lett.* 2012; 108:227801. [PubMed: 23003654]
- [35]. Li B. Continuum electrostatics for ionic solutions with nonuniform ionic sizes. *Nonlinearity*. 2009; 22:811–833.
- [36]. Li B. Minimization of electrostatic free energy and the Poisson–Boltzmann equation for molecular solvation with implicit solvent. *SIAM J. Math. Anal.* 2009; 40:2536–2566.
- [37]. Li B, Liu P, Xu Z, Zhou S. Ionic size effects: generalized boltzmann distributions, counterion stratification, and modified debye length. *Nonlinearity*. 2013; 26:2899–2922. [PubMed: 24465094]
- [38]. Li H, Lu B. An ionic concentration and size dependent dielectric permittivity Poisson–Boltzmann model for biomolecular solvation studies. *J. Chem. Phys.* 2014; 141:024115. [PubMed: 25028007]
- [39]. Lu BZ, Zhou YC. Poisson–Nernst–Planck equations for simulating biomolecular diffusion-reaction processes II: Size effects on ionic distributions and diffusion-reaction rates. *Biophys J.* 2011; 100:2475–2485. [PubMed: 21575582]
- [40]. Lyashchenko AK, Zasetky A. Yu. Complex dielectric permittivity and relaxation parameters of concentrated aqueous electrolyte solutions in millimeter and centimeter wavelength ranges. *J. Molecular Liquids*. 1998; 77:61–75.
- [41]. Ma M, Xu Z. Self-consistent field model for strong electrostatic correlations and inhomogeneous dielectric media. *J. Chem. Phys.* 2014; 141:244903. [PubMed: 25554176]
- [42]. McCammon JA. Darwinian biophysics: Electrostatics and evolution in the kinetics of molecular binding. *Proc. Nat. Acad. Sci. USA*. 2009; 106:7683–7684. [PubMed: 19416830]
- [43]. McLaughlin S. The electrostatic properties of membranes. *Annu. Rev. Biophys. Biophys. Chem.* 1989; 18:113–136. [PubMed: 2660821]
- [44]. Messina R. Electrostatics in soft matter. *J. Phys.: Condens. Matter*. 2009; 21:113102. [PubMed: 21693906]
- [45]. Naji A, Kandu M, Forsman J, Podgornik R. Perspective: Coulomb fluids weak coupling, strong coupling, in between and beyond. *J. Chem. Phys.* 2013; 139:150901. [PubMed: 24160489]
- [46]. Nakamura I, Shi A-C, Wang Z-G. Ion solvation in liquid mixtures: Effects of solvent reorganization. *Phys. Rev. Lett.* 2012; 109:257802. [PubMed: 23368502]
- [47]. Nörtemann K, Hilland J, Kaatz U. Dielectric properties of aqueous NaCl solutions at microwave frequencies. *J. Phys. Chem. A*. 1997; 101:6864–6869.
- [48]. Obolensky OI, Doerr TP, Ray R, Yu Y-K. Rigorous treatment of electrostatics for spatially varying dielectrics based on energy minimization. *Phys. Rev. E*. 2009; 79:041907.
- [49]. Reiner ES, Radke CJ. Variational approach to the electrostatic free energy in charged colloidal suspensions: general theory for open systems. *J. Chem. Soc. Faraday Trans.* 1990; 86:3901–3912.

- [50]. Renou R, Ding M, Zhu H, Szymczyk A, Malfreyt P, Ghoufi A. Concentration dependence of the dielectric permittivity, structure, and dynamics of aqueous NaCl solutions: Comparison between the Drude oscillator and electronic continuum models. *J. Phys. Chem. B.* 2014; 118:3931–3940. [PubMed: 24661006]
- [51]. Sala J, Guàrdia E, Martí J. Effects of concentration on structure, dielectric, and dynamic properties of aqueous NaCl solutions using a polarizable model. *J. Chem. Phys.* 2010; 132:214505. [PubMed: 20528029]
- [52]. Schmidt CC. The dielectric constants of four electrolytes as given by the Carman electrometer method. *Phys. Rev.* 1927; 30:925–930.
- [53]. Sharp KA, Honig B. Electrostatic interactions in macromolecules: Theory and applications. *Annu. Rev. Biophys. Biophys. Chem.* 1990; 19:301–332. [PubMed: 2194479]
- [54]. Sheinerman FB, Norel R, Honig B. Electrostatic aspects of protein-protein interactions. *Curr. Opin. Struct. Biology.* 2000; 10:153–159.
- [55]. Tresset G. Generalized Poisson–Fermi formalism for investigating size correlation effects with multiple ions. *Phys. Rev. E.* 2008; 78:061506.
- [56]. Wang Z-G. Fluctuation in electrolyte solutions: The self energy. *Phys. Rev. E.* 2010; 81:021501.
- [57]. Wei Y, Sridhar S. Dielectric spectroscopy up to 20 GHz of LiCl/H₂O solutions. *J. Chem. Phys.* 1990; 92:923–926.
- [58]. Wei Y-Z, Chiang P, Sridhar S. Ion size effects on the dynamic and static dielectric properties of aqueous alkali solutions. *J. Chem. Phys.* 1992; 96:4569–4573.
- [59]. Wen J, Zhou S, Xu Z, Li B. Competitive adsorption and ordered packing of counterions near highly charged surfaces: From mean-field theory to Monte Carlo simulations. *Phys. Rev. E.* 2012; 85:041406.
- [60]. Xu Z, Ma M, Liu P. Self-energy modified Poisson–Nernst–Planck equations: WKB approximation and finite-difference approaches. *Phys. Rev. E.* 2014; 90:013307.
- [61]. Zhou S, Wang Z, Li B. Mean-field description of ionic size effects with non-uniform ionic sizes: A numerical approach. *Phys. Rev. E.* 2011; 84:021901.

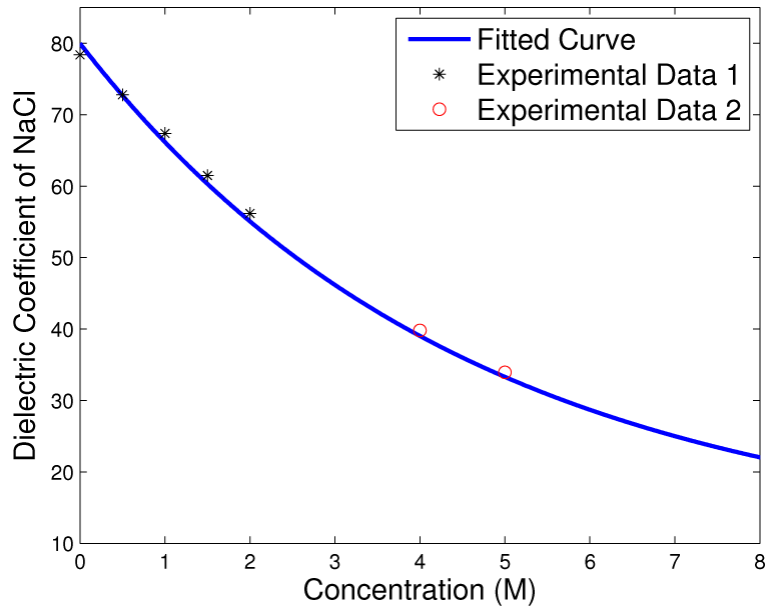


Fig. 1.1. The dielectric coefficient for NaCl solution. The experimental data 1 and 2 are taken from [27] and [40], respectively. The fitted form is $\epsilon\left(\frac{-}{c}\right) = 70e^{-0.22c} + 10$. The maximum relative error at data points is 2%.

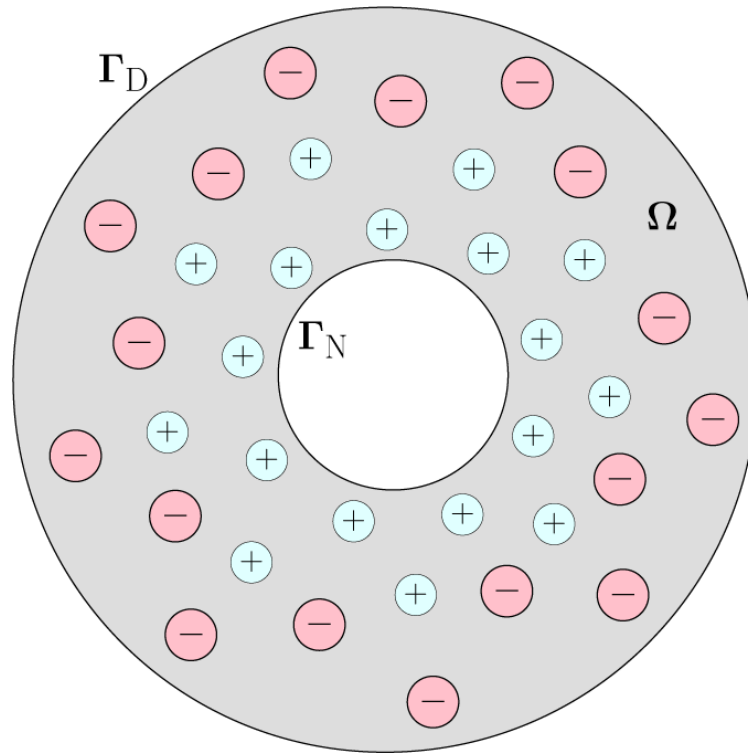


Fig. 1.2.

A schematic view of an ionic solution. The solvent occupies the grey region Ω . Small circles with plus and minus signs represent cations (positively charged ions) and anions (negatively charged ions), respectively.

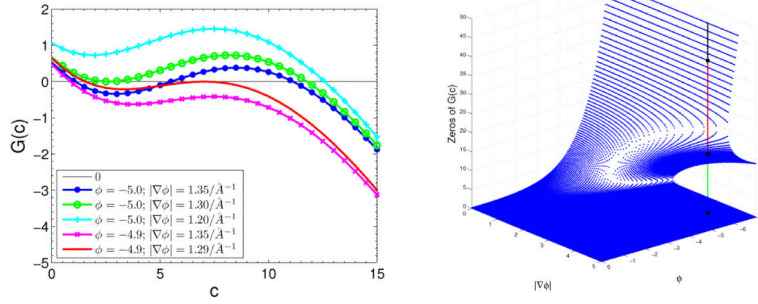


Fig. 4.1. *Left: $G(c)$ vs. c for different values of ϕ and $|\nabla\phi|$. Right: Zeros of $G(c)$ vs. ϕ and $|\nabla\phi|$. The three dots on the vertical line indicate the three zeros of $G(c)$.*

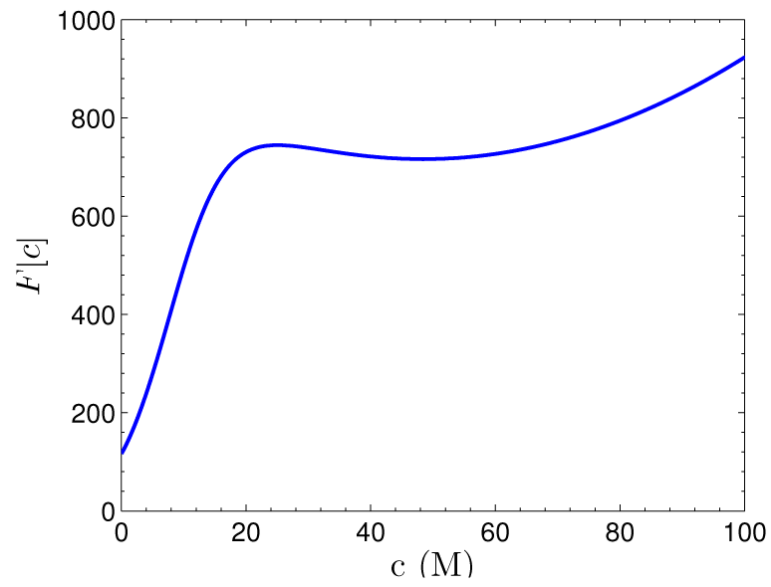


Fig. 4.2.
Graph of the function $F[c]$ defined in (4.3).

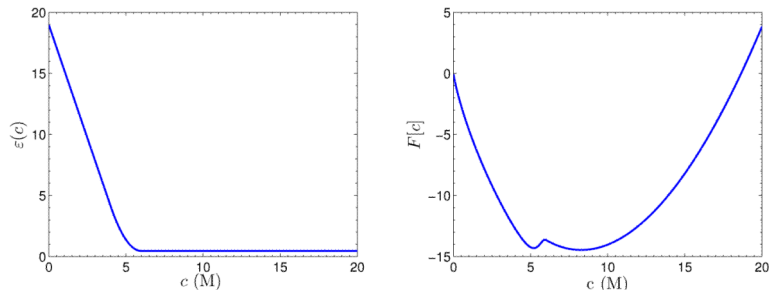


Fig. 4.3.
 Left: Graph of the function $\varepsilon = \varepsilon(c)$ defined in (4.5). Right: Graph of the function $F [c]$ defined in (4.6).

Author Manuscript

Author Manuscript

Author Manuscript

Author Manuscript

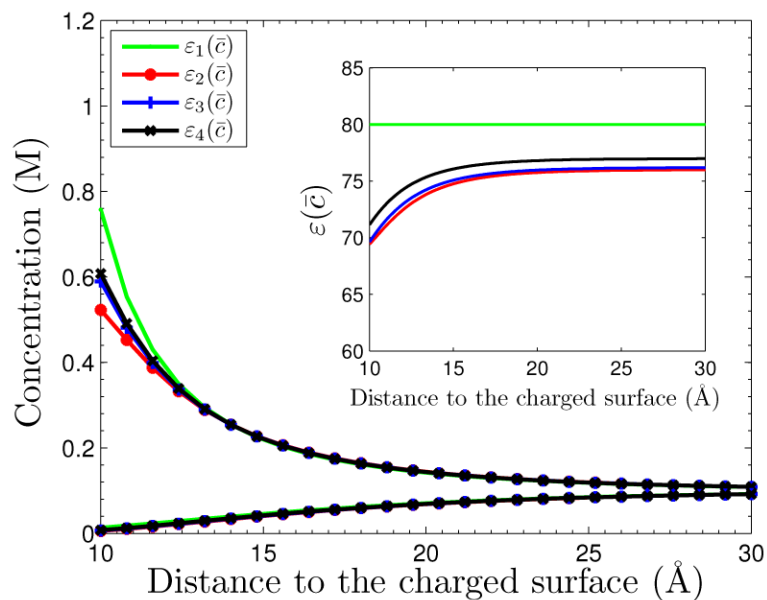


Fig. 5.1. The concentrations vs. radial distance to the charged surface for System I with the surface charge density $\sigma = -0.005 e/\text{\AA}^2$. The four curves with indicated symbols are the counterion concentration profiles. The four coion concentration profiles nearly overlap and become one curve which is the lowest curve. Inset: the graph of function $\varepsilon_i(\bar{c}(r))$ for $i = 1, \dots, 4$.

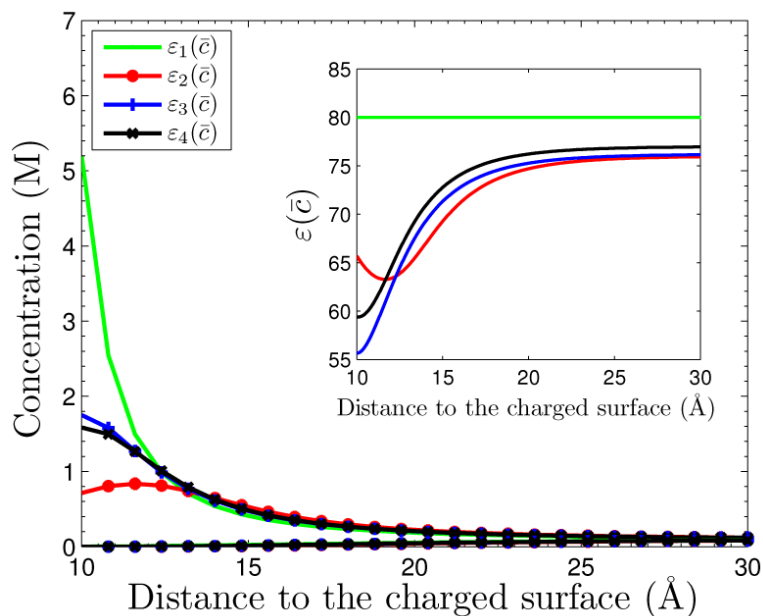


Fig. 5.2. The concentrations vs. radial distance to the charged surface for System I with the surface charge density $\sigma = -0.012 e/\text{\AA}^2$. The four curves with indicated symbols are the counterion concentration profiles. The four coion concentration profiles nearly overlap and become one curve which is the lowest curve. Inset: the graph of function $\varepsilon_i(\bar{c}(r))$ for $i = 1, \dots, 4$.

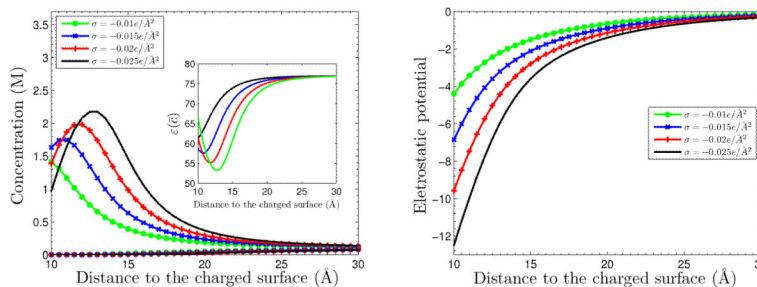


Fig. 5.3.

System I with $\epsilon = \epsilon_4 \left(\frac{-}{c} \right)$. Left: The ionic concentrations vs. the radial distance to the charged surface. The four counterion concentration profiles for the four different values of the surface charge density are indicated by the symbols. The four corresponding coion concentrations overlap and become one curve which is the lowest one. Right: The electrostatic potentials vs. the radial distance to the charged surface for different values of the surface charge density.

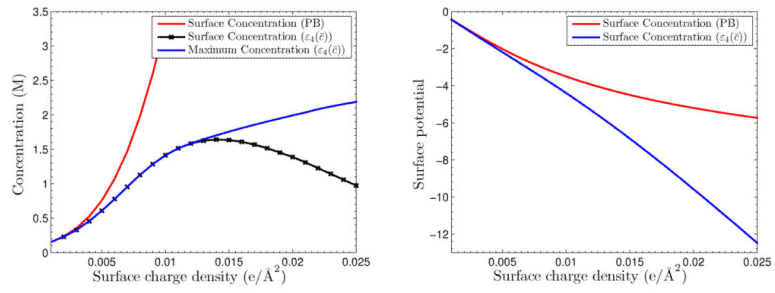


Fig. 5.4.

Left: The Counterion concentration at the charged surface and the maximum value of counterion concentration vs. the surface charge density. Right: The electrostatic potential at the charged surface vs. the surface charge density.

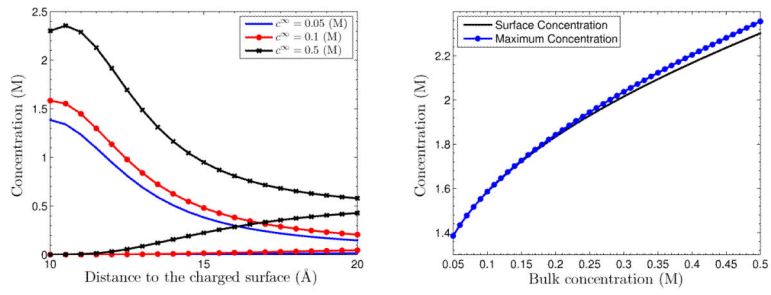


Fig. 5.5. Left: Concentrations vs. radial distance to the charged surface with different ionic concentrations. Right: The counterion concentration at the charged surface and the maximal value of counterion concentration vs. bulk ionic concentration.

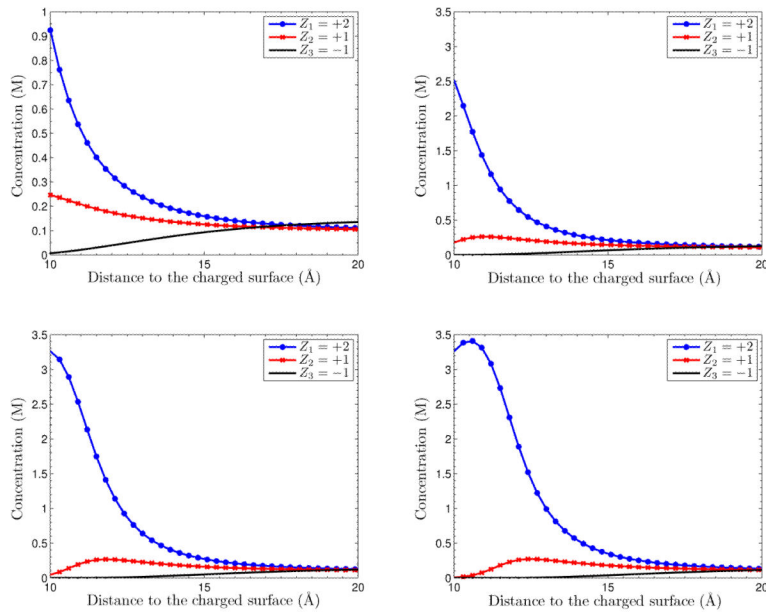


Fig. 5.6. Ionic concentrations vs. radial distance to the charge surface with different values of surface charge density σ . Upper left: $\sigma = -0.005e/\text{Å}^2$. Upper right: $\sigma = -0.01e/\text{Å}^2$. Lower left: $\sigma = -0.015e/\text{Å}^2$. Lower right: $\sigma = -0.02e/\text{Å}^2$.